

## Electrosynthesis and Characterization of Polypyrrole/Cashew Gum Composite Grown on Gold Surface in Aqueous Medium

Rômulo A. O. Castro<sup>1</sup>, Rubênia S. Monte<sup>1</sup>, Luana G. Mendes<sup>1</sup>, Roselayne F. Furtado<sup>2\*</sup>,  
Ângelo R. A. Silva<sup>3</sup>, Atanu Biswas<sup>4</sup>, Huai N. Cheng<sup>5</sup>, Carlucio R. Alves<sup>1\*</sup>

<sup>1</sup> Department of Chemistry, State University of Ceara, 1700 Dr. Silas Munguba Avenue, Fortaleza-CE 60740-903, Brazil.

<sup>2</sup> Embrapa Tropical Agroindustry, 2270 Sara Mesquitaalves Street, Fortaleza-CE 60511-110, Brazil.

<sup>3</sup> Atomic Force Microscopy Laboratory, University of Fortaleza, 1321 Washington Soares Avenue, Fortaleza-CE 60811-905, Brazil.

<sup>4</sup> USDA Agricultural Research Service, National Center for Agricultural Utilization Research, 1815 North University Street, Peoria, Illinois 61604, USA.

<sup>5</sup> USDA Agricultural Research Service, Southern Regional Research Center, 1100 Robert E. Lee Blvd., New Orleans, Louisiana 70124, USA.

\*E-mail: [alvescr@yahoo.com](mailto:alvescr@yahoo.com), [roselayne.furtado@embrapa.br](mailto:roselayne.furtado@embrapa.br)

Received: 15 July 2016 / Accepted: 29 October 2016 / Published: 12 December 2016

---

One of the current trends in the design of electronic materials is the use of agro-based, renewable materials with a minimum amount of toxic substances present. Consistent with this trend, we investigated the electrosynthesis and the electrochemical, morphological, and topographical characteristics of a novel conducting polypyrrole/cashew gum (PPy/CG) composite. The composite films were grown on gold surface by cyclic voltammetry and chronoamperometry in an aqueous medium. They were characterized using FTIR-ATR, SEM, AFM and cyclic voltammetry. The composites gave evidence of the incorporation of CG in PPy film, which had a granular and nodular morphology with grain size ranging from 0.7 to 2.0  $\mu\text{m}$ . Moreover, the films produced by cyclic voltammetry and chronoamperometry carried an anodic load of 3.83 and 4.34  $\text{mC cm}^{-2}$ , respectively. The data also showed that the polypyrrole surface roughness was strongly affected by the CG concentration. This study demonstrated the feasibility of producing an alternative conductive biobased film through electrodeposition of PPy/CG and gave useful information about its structural and electrochemical properties.

---

**Keywords:** composite; polypyrrole; cashew Gum; electrodeposition; conductor.

### 1. INTRODUCTION

The synthesis of new products from renewable materials together with the reduction of the usage of toxic chemical reagents is both a challenge and an opportunity with respect to the

development of novel technologies. Thus, the use of biodegradable materials in electronic products can reduce the accumulation of solid waste and mitigate environmental concerns [1,2]. Furthermore, the ecofriendly materials may have other interesting properties that bring additional benefits to specific applications.

Conducting polymers are excellent materials for use in novel composite materials. Chemical and structural modifications can be made that are related to the variations in oxidation levels. The change that occurs in the charge mobility of the polymer can be easily measured. Polypyrrole (PPy) is a representative conducting polymer and displays interesting electronic properties including conductivity. The conjugated double bonds in its structure allow the flow of electrons along the polymer chain, and the properties of the polymeric film depend on the polymer concentration in the film and the experimental conditions employed for polymer synthesis and film formation. Generally, the combination of polypyrrole/(poly)electrolyte can give a conductive composite that maintains the electrochemical properties of the isolated polymer and improves other properties such as material strength [3]. In view of this perspective, it is of interest to modify a conductive polymer with a biobased material and form films from them, thus opening these composite materials to new applications. In particular, the combination of a polysaccharide and polypyrrole is a promising route that may leverage the benefits of each component polymer and may even provide new features that improve their physical, chemical, mechanical and rheological characteristics [4,5].

The polysaccharides from plants are usually soluble in water and form viscous solutions at moderate concentrations. Cashew gum (CG) obtained from the exudate of *Anacardium occidentale* L. is an acidic heteropolysaccharide composed of galactose main chain and arabinose, glucose, glucuronic acid, mannose and xylose branches [6,7]. The percentages of these monosaccharides vary according to geographic region where the plant is grown and other factors [8]. The easy process of exudation of this gum, its hydrophobicity, biocompatibility and biodegradability are some of its advantages, which should increase the possibility of its commercial production [9]. Previously, multilayer films consisting of cashew gum and polyaniline were assembled by the layer-by-layer technique and used as an electrode for electroanalytical determination of dopamine [10]. A related paper reported the layer-by-layer films made from cashew gum and metallic phthalocyanines [11].

In this work, a polypyrrole-cashew gum composite has been synthesized via potentiostatic and potentiodynamic and characterized by FTIR-ATR, AFM, SEM and electrochemical techniques. To the best of our knowledge, this is the first report of this novel composite. This composite has many desirable properties, such as ease of synthesis, flexibility, large active area, and ready incorporation of different dopant species and biomolecules.

## 2. EXPERIMENTAL

### 2.1. Materials

All solutions were prepared with Milli-Q ultrapure water (18.2 M $\Omega$  cm at 25°C) obtained from Millipore Corporation<sup>®</sup>. Pyrrole (99% Sigma-Aldrich<sup>®</sup>) was purified by distillation (60°C, 50 mmHg) and stored in a dark container at low temperatures. LiClO<sub>4</sub> (Janssen, 99%) was heated at 80°C for 2 hours before use.

## 2.2. Isolation and Physical Chemical Characterization of Cashew Gum (CG)

The gum was collected from *A. occidentale* L. trees grown in the experimental field at Embrapa Tropical Agroindustry, Brazil. The polysaccharide was isolated according to the method described by Torquato et al. [12]. The gum was triturated, dissolved in water, filtered and precipitated with commercial ethanol (96 GL) in a 3:1 (w/w) ratio of ethanol : gum. The precipitate was isolated and dried at 60°C. Afterwards, the gum was crushed in a mill, resulting in a fine white powder. CG was analyzed for ash percentage [13], protein per total nitrogen [14], phenolic compounds [15] and weight-average molecular weight ( $M_w$ ) by gel permeation chromatography (GPC) using a Shimadzu LC-20AD chromatography system with RID-10A refractive index detector.

## 2.3. Electrosynthesis and characterization of composite PPy/CG

The electrochemical cell consisted of three electrodes: a gold disc work electrode ( $\varnothing = 1.6 \text{ mm}^2$ ), a gold disc auxiliary electrode ( $\varnothing = 3.6 \text{ mm}^2$ ), and Ag/AgCl reference electrode. Before each assay, the work electrode was manually polished with alumina to 0.3  $\mu\text{m}$  thickness, followed by cleaning in an ultrasonic bath in 99% ethanol for 10 minutes and thorough rinsing with Milli-Q water. Afterwards, the work electrode was subjected to electrochemical cleaning using cyclic voltammetry in the potential range from -0.2 to 1.4 V (vs. Ag/AgCl) in the presence of 0.5 M  $\text{H}_2\text{SO}_4$  and thorough rinsing with Milli-Q water. The PPy/CG composites were synthesized electrochemically using an Autolab<sup>®</sup> PGSTAT-12 potentiostat/galvanostat controlled by NOVA 1.10 software. The cyclic voltammetry technique was operated with a potential range from -0.5 to 1.0 V (for 20 cycles), a scan rate of 50  $\text{mV s}^{-1}$  and by chronoamperometry at a constant potential of 0.7, 0.8 and 0.9 V for 600 s. In the evaluation of charge storage, the polymer was studied at a  $\text{LiClO}_4$  concentration of 0.1 M, with a potential window from -0.3 to 0.5 V, and a scan rate of 50  $\text{mV s}^{-1}$ .

## 2.4. Microscopy and spectroscopy

The PPy/CG composite was characterized by scanning electron microscopy (SEM, using a Zeiss<sup>®</sup> 940 A microscope, Oberkochen, Germany), Attenuated Total Reflection Fourier transform infrared spectroscopy (FTIR-ATR) (Varian<sup>®</sup> 660-620, Agilent Technologies, Santa Clara, USA), and atomic force microscopy (Agilent 5500 AFM/SPM). AFM was particularly helpful for the investigation of topographic surface through scanning of 10  $\mu\text{m} \times 10 \mu\text{m}$  surface areas. Root mean square (RMS) roughness was used as the parameter to estimate the surface roughness of the materials.

# 3. RESULTS AND DISCUSSION

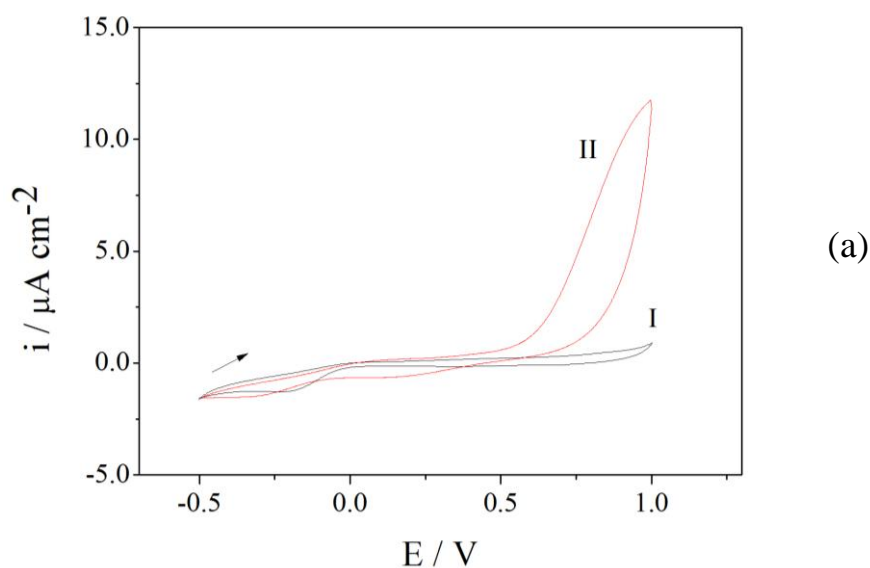
## 3.1. Characterization of CG

The yield of the CG was  $76.07 \pm 2.45\%$ , and the CG seemed to have high purity. The ash content was  $0.7 \pm 0.007\%$ , corroborating the ash content of 0.82% reported by Andrade [16]. The

protein content for isolated CG was  $0.51 \pm 0.07\%$ ; this value was about one-half of the value found by Lima et al. [17], around 1% for the lyophilized gum, which can be rationalized by the presence of residual protein, probably in the arabinogalactan-protein complex (AGP). Therefore, the isolation process performed in this paper was successfully executed. The CG showed a weight-average molecular weight ( $M_w$ ) of  $1.44 \times 10^5 \text{ g mol}^{-1}$ . The knowledge of the molecular weight is relevant, because it is a factor that may affect the conductivity behavior of a polyelectrolyte.

### 3.2. Electrosynthesis of PPy/CG film

For the electrochemical assays, the potential range was set from -0.5 to 1.0 V (Figure 1). The first scan involved CG only, and there was no evidence of degradation (Curve I - Figure 1a). The SEM image for homogeneous film of the polyelectrolyte deposited on gold surface is shown in Figure 1b. PPy/CG composite was electrosynthesized by cyclic voltammetry (Curve II - Figure 1a), where the redox process in the formation of composite was observed. According to Otero et al. [18], the application of a certain potential in the presence of a monomer would produce a free radical, thereby initiating polymerization and subsequent modification of the electrode. In cyclic voltammetry in the presence of Py, there was a shift to higher anodic potential and the formation of a pre-peak at 0.3 V, followed by the high peak at 1.0 V. During successive scans the reversibility of the system was negatively impacted and an increasing separation of the anodic and cathodic potential peaks was observed. The SEM image of PPy/CG (Figure 1c) reveals a morphology typical of granular-like coverage [19]. Thus, a heterogeneous surface with a granular structure and dendrimers was generated. Note that PPy/CG composite had a shiny black color, similar to standard PPy film.



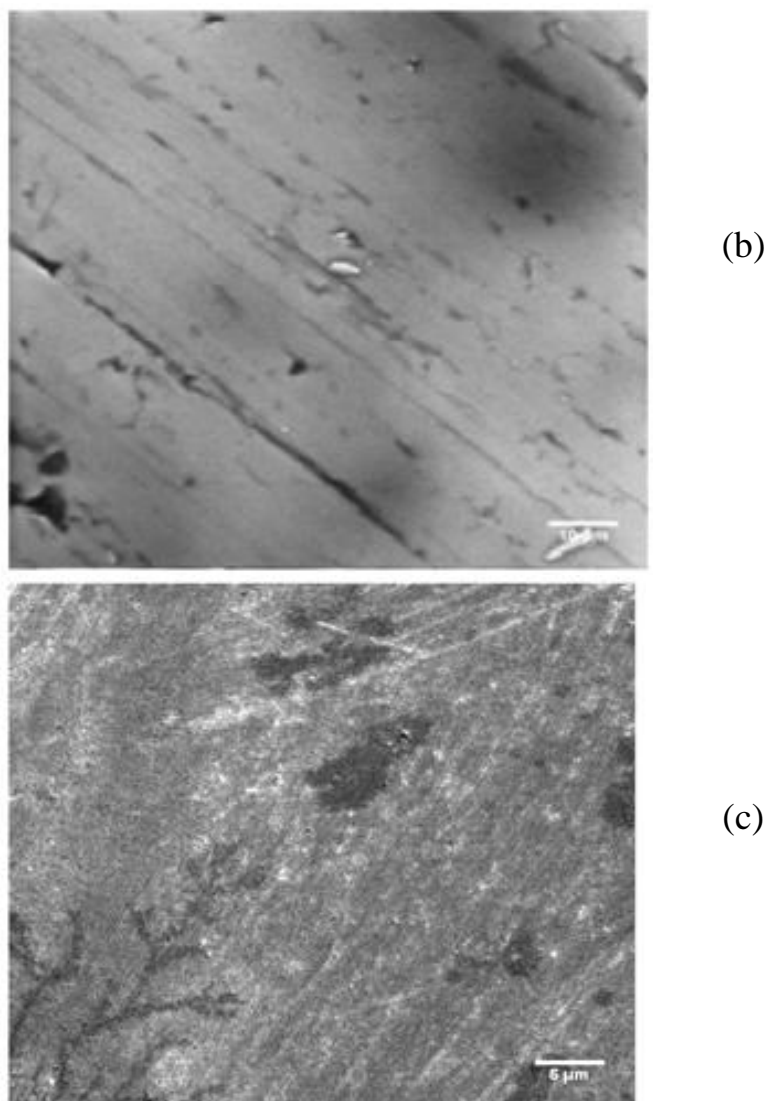


**Figure 1.** (a) Cyclic voltammograms in aqueous medium containing 20% CG (curve I) and [Py] = 0.3 M + 20% CG (curve II) at scan rate of  $50 \text{ mV s}^{-1}$ . (b) SEM micrographs obtained from 20% CG. (c) SEM micrograph obtained for [Py] = 0.3 M + 20% CG films.

The films produced from different concentrations of CG and Py showed higher current peaks for the oxidation process at higher concentrations of Py (Figure 2). The polypyrrole and CG separately have conductive and resistive characteristics, respectively. Thus, we may expect the presence of CG to be disadvantageous to polypyrrole electrosynthesis. However, in this case, CG acts also as a polyelectrolyte during the composite production. At a higher concentration of pyrrole (Figure 2a), 20% CG contributed to an increase in the current peaks for each new cycle. In contrast, at a lower concentration of pyrrole and 20% CG (Figure 2b), for each new cycle of the voltammetric response the current decreased owing the predominance of gum, making the film resistive.

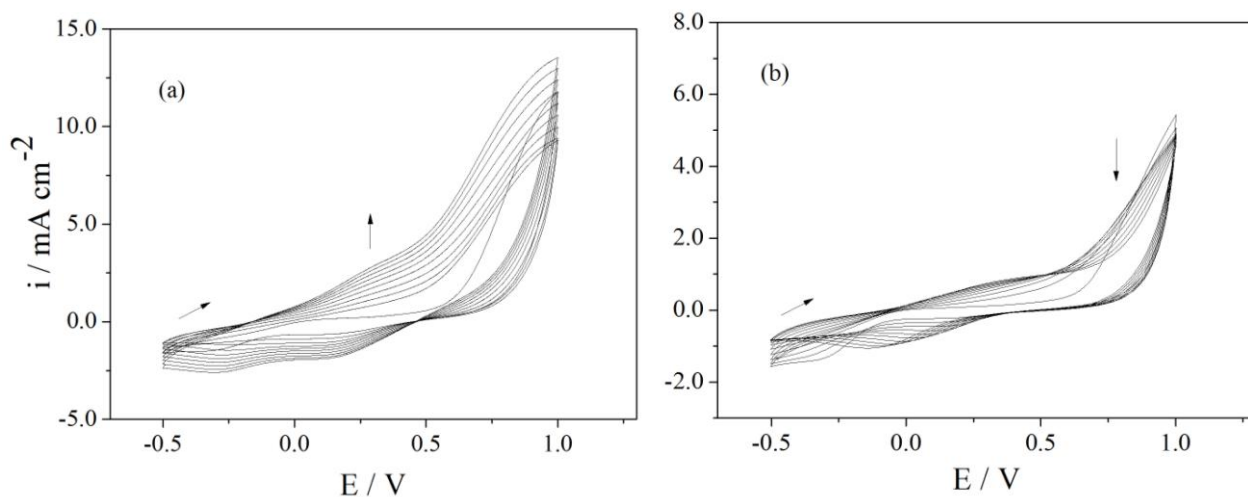


**Figure 2.** Cyclic voltammograms of PPy/CG composites grown in aqueous medium for (a) 20% CG/[Py] = 0.3 M, and (b) 20% CG/[Py] = 0.05 M, at a scan rate of  $50 \text{ mV s}^{-1}$ .

### 3.3. Morphological, spectral, topographic, and electrochemical studies

The charge capacity of the composite was proportional to the charge passed during electropolymerization. The charge grew when a new cycle is performed due to the increase of the superficial area, and the potential peak was shifted in the anodic direction (to give more positive values) which indicated the formation of new layers of PPy/CG composite.

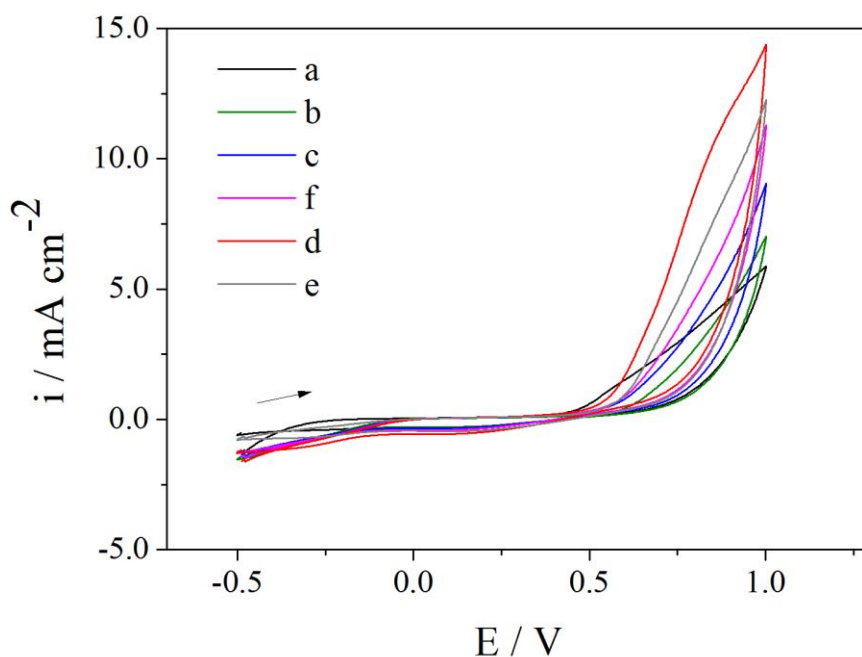


**Figure 3.** Cyclic voltammograms of PPy/CG composite growth in the aqueous medium with  $[\text{Py}] = 0.3 \text{ M}$  in the presence of (a) 1% CG, (b) 5% CG, (c) 10% CG, (d) 20% CG, (e) 30% CG, and (f) 50% CG at a scan rate of  $50 \text{ mV s}^{-1}$ .

Figure 3 shows cyclic voltammograms obtained from 1% to 50% CG and  $[Py] = 0.3$  M. Oxidation of the monomer was observed at different concentrations of CG at  $E_p \approx 0.3$  V. Moreover, the chain density increased with a corresponding increase in CG concentration up to a maximum value of 20%. This fact indicates that ionizable groups from the polyelectrolyte along the chain maintained high ionic strength and promoted electrical conductivity. However, at the highest concentrations, the electroactive area was saturated, thus causing the overlap of the insulating compound in the conductive region. Furthermore, high concentrations of CG might cause conformational changes in PPy chain and hinder the formation of dimers and trimers during the oxidation process of the Py.

At low concentrations of Py, there was the formation of the composite that produced modest undercurrent peaks. This was associated with the subtle efficiency of incorporation of the CG into films. When the composites were produced at higher concentrations of Py (e.g., 0.3 M of Py), it was observed that the incorporation of up to 30% CG increased considerably the current peaks. From experiments using different concentrations, it could be concluded that  $[Py] = 0.3$  M together with 20% CG performed better for the formation of the conductive composite.

Figure 4 shows the chronoamperometric data of current responses versus time during the process of electrosynthesis of PPy/CG on gold electrode in the aqueous medium. At low concentrations of CG, there was a slight increase of the current indicating a low level of film formation. Stabilization in the current plateau was observed at different concentrations of CG up to 20%-30% CG. Degradation of the composite formed was observed at electric potentials higher than 1.1 V. Thus, the process of electrosynthesis of PPy/CG by chronoamperometry may be described in three steps: at the initial stage abrupt reduction of the current occurs on gold surface associated with the formation of the first layer of conductive composite, followed by increasing current rate due to the increase in surface area (a result of film growth), and then stabilization during which the film growth rate and the current stays constant.

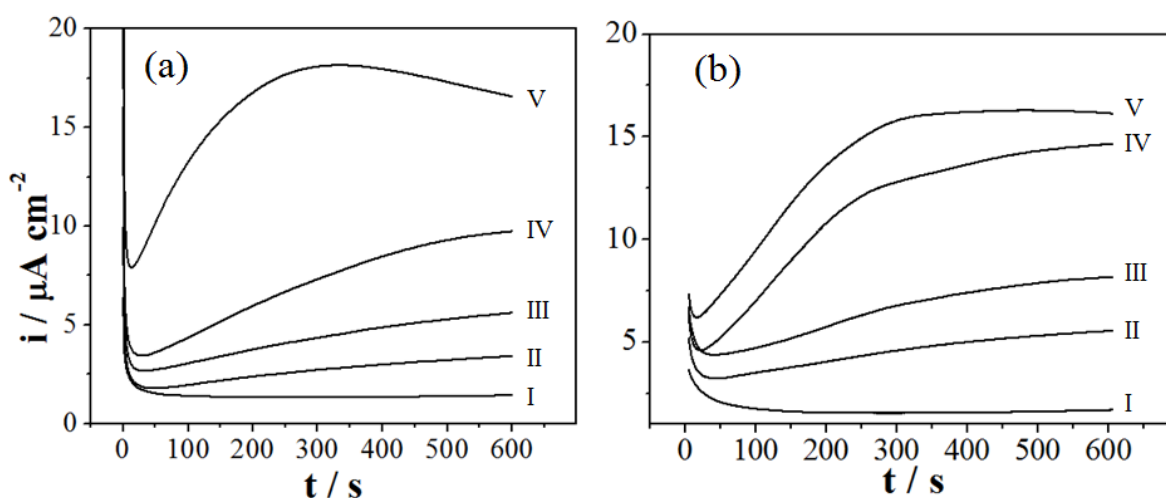


**Figure 4.** Chronoamperograms of PPy/CG composite growth in aqueous medium with (a)  $E_p = 0.8$  V, and (b) 0.9 V, for  $[Py] = 0.3$  M and CG: 1% (I), 5% (II), 10% (III), 20% (IV), and 30% (V).

FTIR-ATR analysis was performed on the composites grown potentiostatically and potentiodynamically (Figure 5). The spectrum of samples produced by the potentiostatic method

(Figure 5a) had higher intensities of peaks, indicating that the amount of film formed was greater. The composite spectrum contained all the characteristic peaks for CG and pyrrole ring. Pyrrole polymerization was confirmed with the peaks at  $3420\text{ cm}^{-1}$  due to N-H stretch associated with secondary amines, while  $1569$ ,  $1463$  and  $1023\text{ cm}^{-1}$  peaks were related, respectively, to stretching of C=C, C=N and N-H groups on the pyrrole ring [20]. The presence of CG in the composite was evidenced by the large deformation band at  $3400\text{ cm}^{-1}$ , due to OH stretching vibration (characteristic of carbohydrates) and  $2925$  and  $2854\text{ cm}^{-1}$  bands that corresponded to symmetric and asymmetric CH stretching from primary and secondary carbon and  $1460\text{ cm}^{-1}$  from angular deformation of C-H. The secondary alcohols were identified via the  $1264$  and  $1060\text{ cm}^{-1}$  bands, due to symmetrical and asymmetrical deformations of C-O and the presence of a strong peak at  $1157\text{ cm}^{-1}$  related to secondary alcohol [21].

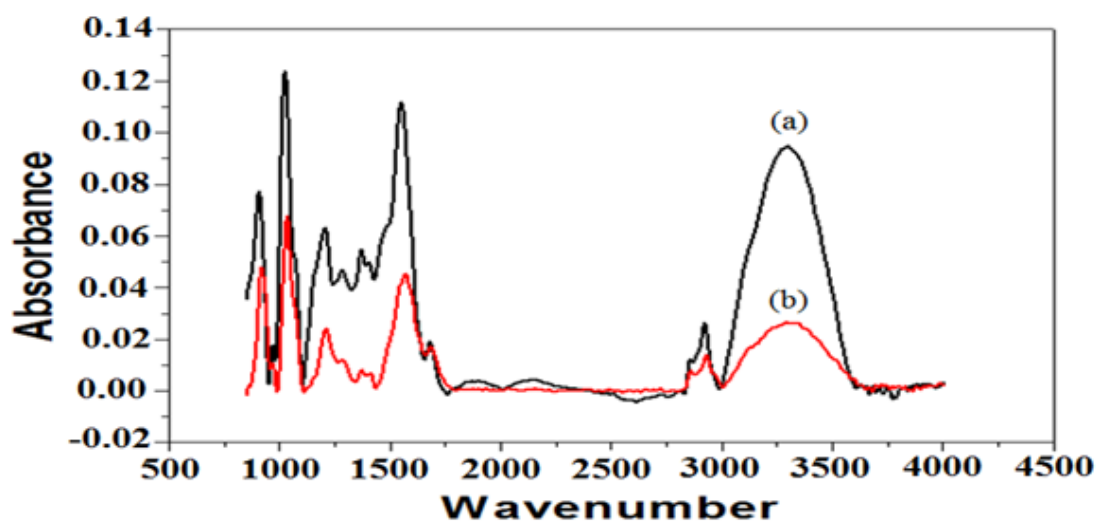


**Figure 5.** FTIR-ATR spectra of PPy/CG films prepared with  $[\text{Py}] = 0.3\text{ M}$ / 20% CG in aqueous medium and obtained at (a)  $E_p = 0.8\text{ V}$ , and (b) cyclic voltammetry with scan rate =  $50\text{ mV s}^{-1}$ .

The film load transfer was studied for the different electrosynthesis techniques in a potential range where there was no redox occurring in the PPy/CG film. The experiment aims to analyze the intercalation of ions in the composite (Figure 6). The retention process is known as doping, and there is insertion of ions, such as lithium, onto the polymer chain. The charge transfer engenders modifications in the electronic distribution of the polymer, giving rise to the electronic states located between the valence band and the conduction band (called energy gap). The charge carriers responsible for electronic conduction in the polymer are the polarons and the bipolarons. Thus, conduction is associated with the movement of these carriers along the chain, performing rearrangement of single and double bonds at different resonance modes.

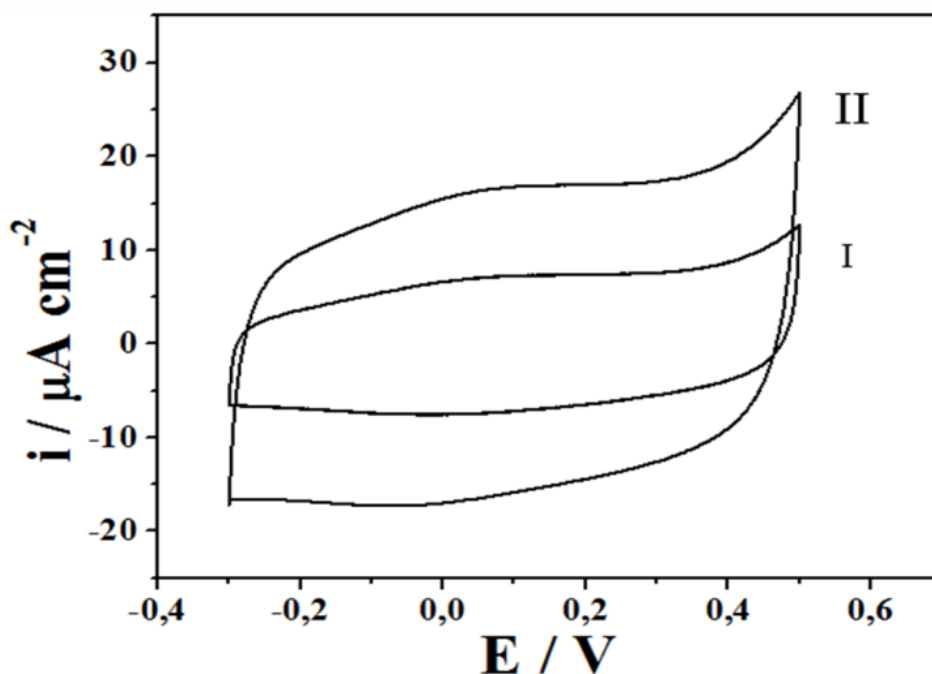


**Figure 6.** Cyclic voltammograms in aqueous medium with  $[\text{LiClO}_4] = 0.1 \text{ M}$  at a scan rate of  $20 \text{ mV s}^{-1}$  for  $[\text{Py}] = 0.3 \text{ M}/20\% \text{ CG}$  composites grown by (I) cyclic voltammetry, and (II) chronoamperometry at  $E_p = 0.8 \text{ V}$  for 600 s.

The evaluation of the charge storage capacity of the PPy/CG composite was performed using  $[\text{LiClO}_4] = 0.1 \text{ M}$  as an electrolyte and a potential window from  $-0.3$  to  $0.5 \text{ V}$ . According to Figure 6, the anodic charge of the growth composite by cyclic voltammetry (curve I) in the potential range from  $-0.5$  to  $1.0 \text{ V}$  (for 20 cycles) and a scan rate of  $50 \text{ mV s}^{-1}$  was  $3.83 \text{ mC cm}^{-2}$ , while the anodic charge for the composite obtained by chronoamperometry (curve II), at fixed potential of  $0.8 \text{ V}$  for 600 s, was  $4.34 \text{ mC cm}^{-2}$ . This result was expected because films grown at fixed potential, in general, are thicker and do not favor monomer oxidation on the polymeric film.

The electroadsorption of PPy/CG films is influenced by the application of electrical potential; in turn, the amount deposited also depends on the time of deposition. The potential applied determines the speed of the reaction and consequently the structure of the adsorbed layer. In the cyclic voltammograms (Figure 7) a gradual increase in  $i_p$  intensity was observed due to the increase in scan rate. The linearity between the  $i_p$  strength and the square root of the potential scan rate ( $v^{1/2}$ ) given by equation,  $i_p \text{ (A)} = 2.66 \times 10^{-7} + 2.15 \times 10^{-6} (v^{1/2})$ , with  $R^2 = 0.977$ , indicates that the transport mechanism was dominated by diffusion. This means that the film has promising capacitive properties of electric storage and dissipation and potential use in the development of electronic devices.

AFM technique was used to examine roughness and topography of films grown potentiostatically and potentiodynamically. The surface image of PPy/CG composites is shown in Figure 8. The surfaces are indeed rough but there are differences between the films.

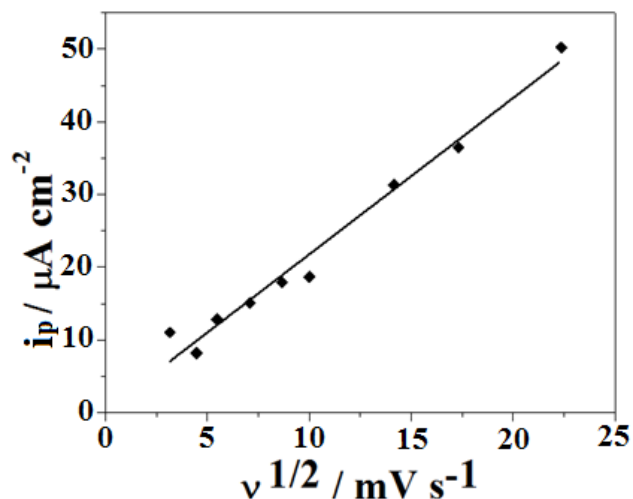


**Figure 7.** Plot of  $i_{\text{peak}}$  vs. scan rate as obtained for  $[\text{Py}] = 0.3 \text{ M}$ / 20% CG composite in aqueous medium by cyclic voltammetry with a scan rate of  $50 \text{ mV s}^{-1}$ .

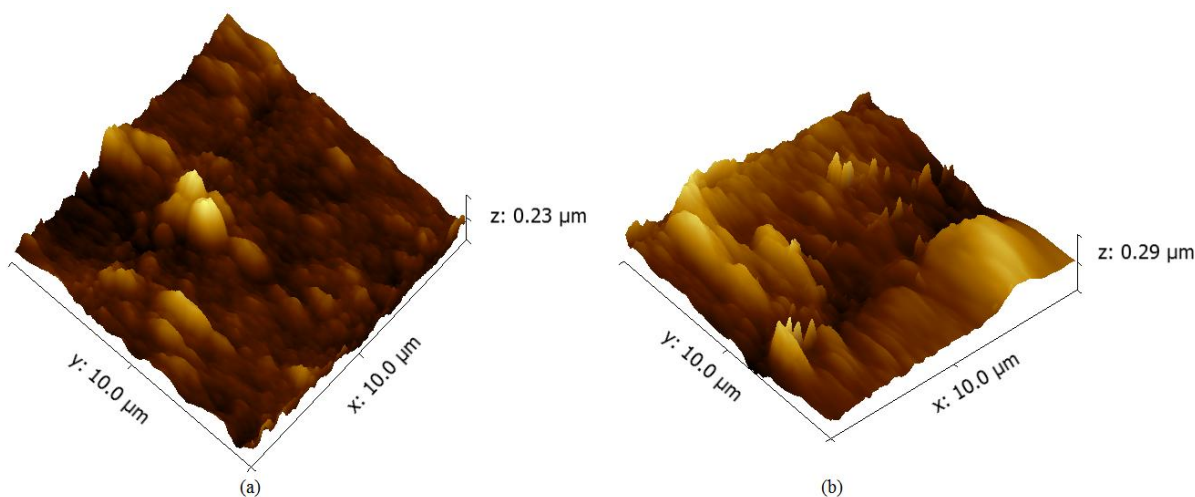


**Figure 8.** AFM images of PPy/CG composite prepared on gold surface with  $[\text{Py}] = 0.3 \text{ M}$ / 20% CG prepared in aqueous medium: (a) by potentiodynamic electrosynthesis at a scan rate of  $50 \text{ mV s}^{-1}$  and (b) by potentiostatic electrosynthesis,  $E_p = 0.8 \text{ V}$  for 600 s.

PPy/CG composite had a granular and nodular morphology with grain size ranging from 0.7 to  $2.0 \mu\text{m}$ . The two types of composites were less rough than pure PPy film, probably due to the effect of PPy/CG structure (Table 1). The surface roughness parameters were expressed as root mean square (RMS) values. The RMS surface roughness values of PPy/CG composite obtained by potentiodynamic and potentiostatic electrosynthesis were 17.2 nm and 9.5 nm, respectively. The data show that the composite surface is smoother than the polypyrrole surface. Moreover, the roughness of the film formed by PPy/CG is greater than the films produced only by using CG. In view of these observations, the composite should be a suitable platform for the adsorption of biomolecules.

**Table 1.** Surface roughness parameters of CG, PPy, and PPy/CG composite films from AFM.

	Roughness parameters		
	Sa (nm)	Sq (nm)	Sz (nm)
Pure CG	1.9	3.6	24.0
Pure Py	21.9	34.1	107.3
PPy/CG <sup>(a)</sup>	11.0	17.2	61.9
PPy/CG <sup>(b)</sup>	6.4	9.5	52.9

<sup>a</sup> Composites obtained by potentiodynamic electrosynthesis at scan rate of 50 mV s<sup>-1</sup>

<sup>b</sup> Composites made by potentiostatic electrosynthesis at E<sub>p</sub> = 0.8 V for 600 s.

#### 4. CONCLUSION

In this work, direct electrogeneration of PPy/CG composite by cyclic voltammetry or chronopotentiometry in aqueous solutions was demonstrated. The composite properties depended on the pyrrole and the cashew gum concentrations in the solution. The novel composites grown potentiostatically and potentiodynamically exhibited different morphological, topographical and electrochemical characteristics when compared with polypyrrole. These composites also provided well-defined redox properties. It was found that the composite formed through the use of a fixed electrochemical potential demonstrated even better conductive properties. Thus, an electrode modified with the conductive film offers several advantages due to the increase in the electroactive area and the improvements in its physical and chemical properties (e.g., the possibility of obtaining ordered molecular structure), thereby making it possible to optimize the complexation and/or electron transfer process.

#### ACKNOWLEDGMENTS

The authors would like to thank the Brazilian agencies, CNPq, FUNCAP and CAPES, for their financial support and Embrapa Tropical Agroindustry and National Center of Energy and Materials Research (CNPEM) for collaborations that resulted in this research. Mention of trade names or commercial products in this publication is solely for the purpose of providing specific information and does not imply recommendation or endorsement by the U.S. Department of Agriculture. USDA is an equal opportunity provider and employer.

#### References

1. S. Musson, K. Vann, Y. Jang, S. Mutha, A. Jordan, B. Pearson and T. Townsend, *Environ. Sci. Technol.*, 40 (2006) 2721.
2. Q. Liu, J. Cao, K. Q. Li, X.H. Miao, G. Li, F.Y. Fan and Y.C. Zhao, *Environ. Sci. Pollut.*, 16 (2009) 329.
3. C.R. Alves, P. Herrasti, P. Ocón, L.A. Avaca and T.F. Otero, *Polym. J.*, 33 (2001) 255.
4. Z. Liu, Y. Jiao, Y. Wang, C. Zhou and Z. Zhang, *Adv. Drug Deliver. Rev.*, 60 (2008) 1650.

5. R.S. Monte, L.R.V. Kotzebue, D.L. Alexandre, R.F. Furtado, J.A.C. Santos, J.D.P. Dantas and C.R. Alves, *J. Brazil. Chem. Soc.*, 25 (2014) 597.
6. B.C. Porto, P.E.D. Augusto, A. Terekhov, B.R. Hamakerc and M. Cristianini, *Carbohydr. Polym.*, 129 (2015) 187.
7. R.C.M., Paula and J.F., Rodrigues, *Carbohydr. Polym.*, 26 (1995) 177.
8. L.A. Sarubbo, L.A. Oliveira, A.L.F. Porto, H.S. Duarte, A.M.A. C. Leao, J.L.L. Filho, G.M.C. Takaki and E.B. Tambourgi, *J. Chromatogr. B Biomed. Sci. Appl.*, 743 (2000) 79.
9. M.G. Carneiro-da-Cunha, M.A. Cerqueira, B.W.S. Souza, M.P. Souza, J.A. Teixeira and A.A. Vicente, *J. Food Eng.*, 95 (2009) 379.
10. S. B. Araujo Barros, C. M. da Silva Leite, A. C. F. de Brito, J. R. dos Santos Jr, V. Zucolotto and C. Eiras, *Int. J. Anal. Chem.*, 2012, Article ID 923208. doi:10.1155/2012/923208
11. I. M. S. Araújo, M. F. Zampa, J. B. Moura, J. R. dos Santos Jr., P. Eaton, V. Zucolotto, L.M.C. Veras, R.C.M. de Paula, J.P.A. Feitosa, J.R.S.A. Leite, and C. Eiras, *Mat. Sci. Engineering: C*, 32 (2012), 1588.
12. D.S. Torquato, M.L. Ferreira, G.C. Sá, E.S. Brito, G.A. S. Pinto and E.H.F. Azevedo, *J. Microbiol. Biotechn.*, 20 (2004) 505.
13. W. Horwitz. Official methods of analysis of the AOAC international. Gaithersburg (2005).
14. W.E. Baethgen and M.M. Alley, *Commun. Soil Sci. Plan. Anal.*, 20 (1989) 961.
15. J.P. Jiménez and F.S. Calixto, *Int. J. Food Sci. Tech.*, 43 (2008) 185.
16. K.C.S. Andrade, C.W.P. Carvalho, C.Y. Takeiti, H.M.C. Azeredo, J.S. Corrêa and C.M. Caldas, *Polimeros*, 23 (2013) 667.
17. R.D.N. Lima, J.R. Lima, C.R. Salis and R.A. Moreira, *Biotechnol. Appl. Bioc.*, 35 (2002) 45.
18. T.F. Otero, P. Herrasti, P. Ocón and C.R. Alves, *Electrochim. Acta*, 43 (1998) 1089.
19. J. Arjomandi, D. Raoufi and F. Ghamari, *J. Phys. Chem. C*, 120 (2016), 18055.
20. K. M. Cheung, D. Bloor and G.C. Stevens, *Polymer*, 29 (1988) 1709.
21. P.L.R. Cunha, J.S. Maciel, M.R. Sierakowski, R.C.M. Paula and J.P.A. Feitosa, *J. Brazil. Chem. Soc.*, 18 (2007) 85.